Developmental Biology 388 (2014) 22–34

Contents lists available at ScienceDirect

Developmental Biology

journal homepage: www.elsevier.com/locate/developmentalbiology

Prenatal exposure to chromium induces early reproductive senescence by increasing germ cell apoptosis and advancing germ cell cyst breakdown in the F1 offspring

Kirthiram K. Sivakumar [a], Jone A. Stanley [a], Joe A. Arosh [a], Melissa E. Pepling [b], Robert C. Burghardt [a], Sakhila K. Banu [a,*]

[a] Department of Integrative Biosciences, College of Veterinary Medicine and Biomedical Sciences, TAMU-4458, Texas A&M University, College Station, TX 77843, USA
[b] Department of Biology, Syracuse University, 114 Life Sciences Complex, 107 College Place, Syracuse, NY 13244, USA

ARTICLE INFO

Article history:
Received 22 November 2013
Received in revised form
21 January 2014
Accepted 4 February 2014
Available online 12 February 2014

Keywords:
Ovary
Chromium
Primordial follicle
Germ cell cyst breakdown
Follicle atresia

ABSTRACT

Hexavalent chromium (CrVI), one of the more toxic heavy metals, is widely used in more than 50 industries such as chrome plating, welding, wood processing and tanneries. As one of the world's leading producers of chromium compounds, the U.S. is facing growing challenges in protecting human health against multiple adverse effects of CrVI. CrVI is rapidly converted to CrIII intracellularly, and can induce apoptosis through different mechanisms. Our previous studies demonstrated postnatal exposure to CrVI results in a delay or arrest in follicle development and puberty. Pregnant rats were treated with 25 ppm potassium dichromate (CrVI) from gestational day (GD) 9.5 to 14.5 through drinking water, placentae were removed on GD 20, and total Cr was estimated in the placentae; ovaries were removed from the F1 offspring on postnatal day (PND)-1 and various analyses were performed. Our results show that gestational exposure to CrVI resulted in (i) increased Cr concentration in the placenta, (ii) increased germ cell apoptosis by up-regulating p53/p27–Bax–caspase-3 proteins and by increasing p53–SOD-2 co-localization; (iii) accelerated germ cell cyst (GCC) breakdown; (iv) advanced primordial follicle assembly and primary follicle transition and (v) down regulation of p-AKT, p-ERK and XIAP. As a result of the above events, CrVI induced early reproductive senescence and decrease in litter size in F1 female progeny.
Published by Elsevier Inc.

Introduction

Striking findings from clinical and epidemiological studies in the past decade indicate that detection of endocrine disrupting chemicals in the human serum, seminal plasma, and follicular fluid of women is directly connected with infertility problems in couples (Marques-Pinto and Carvalho, 2013). Hexavalent chromium (CrVI) is a heavy metal endocrine disruptor (Barceloux, 1999). Environmental contamination with CrVI is a major threat to human health and has been increasing due to the wide range of industrial uses of chromium globally (Banu, 2013). People living in more than 7000 communities in the U.S. drink tap water contaminated with Cr (Sutton, 2010). Significant contamination with CrVI has been detected in the drinking water in California (Salnikow and Zhitkovich, 2008), Texas (Honeycutt, 2010), Chicago (Hawthorne, 2011) and more than 30 other cities in the USA (Layton, 2010). The US EPA approved level for total Cr is 100 μg or 0.1 mg/L). However, Cr levels in drinking water in developing countries range from 0.8 mg (Tokyo, Japan) to 31 mg (Faridabad, India) (Banu et al., 2008). The health risk assessment of CrVI has largely been based on data from occupationally exposed people, although little attention has been given to reproductive and developmental effects. Women working in Cr industries and living around Cr-contaminated environments experience various reproductive problems such as abnormal menses, infertility, stillbirth, and increased postpartum bleeding which are accompanied by high Cr levels in blood and urine (Greene et al., 2010; Jendryczko et al., 1984; Shmitova, 1980; Zhang et al., 1992). Cr can also be transported to the offspring of pregnant women exposed to high levels of Cr (Barceloux, 1999). Cr is transferred through the placenta to developing fetuses (Ziaee et al., 2007) and impairs embryonic development, implantation, fetal viability, and reproductive functions in the F1 generation in rats (Kanojia et al., 1998), although the mechanisms remain unknown.

Primordial germ cells arrive at the gonad and divide to form germ cell cysts (GCC); eventually GCCs break apart and become

* Corresponding author. Fax: +1 979 847 8981.
E-mail address: skbanu@cvm.tamu.edu (S.K. Banu).

http://dx.doi.org/10.1016/j.ydbio.2014.02.003
0012-1606 Published by Elsevier Inc.

surrounded by granulosa cells to form primordial follicles. In most mammals, primordial follicles form either before or during the first few days after birth (Pepling, 2012a). Two-thirds of the germ cells die prior to the primordial follicle assembly (Pepling, 2012b). The ultimate number of primordial follicles determines the lifetime follicle reserve, as the follicle pool determines fertility (Maheshwari and Fowler, 2008). Defects in either the timing or process of GCC breakdown can result in improper primordial follicle assembly or accelerated atresia and thus lead to early reproductive senescence or infertility. Recent findings documented that prenatal exposure to progesterone, and isoflavonoid phytoestrogen, genistein, inhibited GCC breakdown and primordial follicle assembly in mice (Chen et al., 2007). In particular, neonatal exposure to genistein resulted in multi-oocyte follicles in the ovary of PND 19 mice, which was mediated through ERβ (Jefferson et al., 2006).

The mechanism of germ cell death and/or primordial follicle atresia during development of the fetal and neonatal ovary is not well understood. There are reports of non-classical apoptotic phenotypes such as necrotic or autophagic cell death (De Felici et al., 2008; Wartenberg et al., 2001). Several lines of evidence in the different strains of mouse indicate caspase-3-independent primordial follicle atresia (Fenwick and Hurst, 2002; Tingen et al., 2009b). Therefore, there is a critical need to study the mechanism of germ cell death, not only during the normal development of the ovary, but also in response to exposure with EDCs.

PI3K/AKT signaling is a critical regulator of oogenesis (Cecconi et al., 2012; Edson et al., 2009; Rodrigues et al., 2008). Deletion of AKT causes infertility and premature ovarian failure (POF) indicating an essential role in preserving the normal female reproductive lifespan (Edson et al., 2009). Expression of X-linked inhibitor of apoptosis protein (XIAP) in cultured rat granulosa cells was reported to be increased following treatment with TGFα or FSH; and transient over-expression of XIAP was found to inhibit TNFα-induced apoptosis (Wang et al., 2002; Xiao et al., 2001). Interestingly, levels of IAPs were minimal or non-detectable in follicles actively undergoing atresia in both the rat and hen ovaries, while their expression was dramatically elevated in granulosa cells from healthy pre-ovulatory follicles compared to undifferentiated atretic follicles from the hen (Johnson et al., 1998). However, role of AKT or XIAP is not understood in GCC breakdown either under normal conditions or in response to endocrine disrupting chemical exposure.

In addition to potential contributions of AKT and caspase-3 pathways, our previous findings revealed that p53 is a major pathway through which CrVI induces granulosa cell apoptosis (Banu et al., 2011). CrVI increases mitochondrial translocation of p53 that preceeds apoptosis in granulosa cells (Banu et al., 2011). Activation of p53 leads to cell growth arrest, senescence or apoptosis (Yamakuchi and Lowenstein, 2009). In addition, p53 is directly translocated to mitochondria and forms complexes with the Bcl-XL and Bcl-2 proteins, increases permeabilization of the outer mitochondrial membrane, facilitates release of cytochrome *c*, and activates caspase-3 to induce apoptosis (Haupt et al., 2003a; Haupt et al., 2003b). When cells are exposed to oxidative stress, toxicants, DNA damage and hypoxia signals, p53 protein is stabilized, activated and transported into nucleus and induces apoptosis (Giaccia and Kastan, 1998). However, there is no report of the role of p53 in fetal ovarian development.

Therefore, we hypothesize that *in utero* exposure to CrVI causes early reproductive senescence by increasing germ cell death, advancing germ cell cyst breakdown, accelerating primordial follicle atresia, and promoting primordial follicle transition into primary follicles. The objectives were to (i) determine effects of *in utero* exposure to CrVI on pregnancy rate and litter size in the F1 offspring; (ii) evaluate the role of CrVI on GCC breakdown; (iii) understand the role of CrVI on primordial follicle assembly and atresia; (iv) assess the effects of CrVI on the cell survival machinery such as p-AKT, p-ERK and XIAP; and (v) explore the mechanism of p53 in CrVI-induced germ cell apoptosis via caspase-3, GCC breakdown, and primordial follicle assembly.

Materials and methods

In vivo dosing of the animals and experimental design

Pregnant rats of 60–70 days of age were divided into two groups: *Group* 1 – Control ($n=15$) and *Group* 2 – CrVI ($n=15$). Control rats received regular drinking water and diet *ad libitum*. Rats from the CrVI group received 25 ppm potassium dichromate in drinking water from gestational day (GD) 9.5–14.5. The first set of control ($n=5$) and CrVI ($n=5$) treated rats were euthanized on GD 20, and placentae were removed to estimate chromium levels. The second set of rats ($n=5$) was allowed to deliver pups. When the pups were born, ovaries were removed from pups on postnatal day (PND)-1 for further analyses. The third set of rats ($n=5$) was maintained with their F1 female offspring and provided with regular drinking water and diet *ad libitum* until weaning on PND-22. After weaning, the F1 female pups were maintained separately and fed with regular diet and drinking water. On PND-60, F1 offsprings from control ($n=15$) and CrVI-treated ($n=15$) rats were allowed to mate with normal fertility-proven male rats. Appearance of vaginal plug or presence of sperm in the vaginal lavage was considered on 0.5 day of pregnancy. Soon after the birth of F2 offsprings, the offsprings were removed and mothers (F1) were allowed to return to the estrous cycle to be mated again. The percentage of F1 females that achieved successful pregnancy and the number of pups/litter were calculated at 2–4, 4–6, 6–8 and 8–10 months of age.

Estimation of placental chromium

Total Cr levels in the placenta were estimated by mass spectroscopy on a PerkinElmer DRC II instrument (PerkinElmer Life and Analytical Sciences, Shelton, CT) by the Trace Element Research Laboratory (TERL) core facility, College of Veterinary Medicine and Biomedical Sciences, Texas A&M University, based on the standard protocol.

Histology

Histological processing of the ovary was performed by the Histology Core Lab Facility, College of Veterinary Medicine, Texas A&M University, based on the standard protocols for paraffin-embedded sections that were cut at 5 μm thickness and stained with hematoxylin and eosin.

TUNEL assay

Paraffin-embedded tissue sections were deparaffinized in xylene and dehydrated in a graded ethanol series: 90%, 80%, and 70% for 3–6 min, followed by washing in double distilled water. Nuclei of tissue sections were stripped of proteins by incubating with 20 μg/ml proteinase K (in 200 ml of 10 mM Tris–HCl, pH 7.4) for 30 min at 21–37 °C, and washed in PBS. Endogenous peroxidase was inactivated by incubating sections with 3% H_2O_2 in methanol for 10 min at room temperature (RT), blocked with 3% BSA in PBS for 30 min, and washed in PBS. For the positive control, sections were incubated with DNase I (diluted in 50 mM Tris–HCl, pH 7.5, 10 mM $MgCl_2$, and 1 mg/ml BSA) for 10 min at 22 °C to induce DNA strand breaks. Slides were rinsed twice in PBS

followed by the addition of 50 μl of TUNEL reaction mixture to the sections followed by incubation for 60 min at 37 °C in a humidified chamber in the dark. The sections were rinsed and incubated with the TUNEL detection antibody (Roche) labeled with peroxidase. The peroxidase was visualized with diaminobenzidine. Slides were mounted and analyzed by light microscopy. The intensity of staining for each protein was quantified in 10 randomly selected high power fields from each experimental group, using Image-Pro Plus software (Media Cybernetics, Bethesda, MD) as described previously (Banu et al., 2009; Stanley et al., 2013) according to the manufacturer's instructions.

Whole mount fluorescence immunohistochemistry, analysis of germ cell cyst breakdown and follicle development

Ovaries were dissected out, washed in PBS and fixed with 5.3% formaldehyde (Cat#18814, Polysciences) overnight at 4 °C. The ovaries were washed for 30 min in PBS+0.1% Triton-X-100 (PT) and incubated in PT+5% BSA for 1 h at RT. They were then labeled with primary antibodies at an appropriate dilution in PT+5% BSA by incubating overnight at 4 °C. Then the ovaries were washed in PT+1% BSA for 30 min at RT, incubated in RNase A (5 μl of 20 mg/ml RNase A in 1 ml PT+1% BSA, Cat# 12091-039, Life Technologies, Carlsbad, CA) for 30 min. Further, the tissues were incubated with fluorophore-conjugated secondary antibodies in PT+5% BSA for 4 h at RT. Then the tissues were washed 3 times in PT+1% BSA for 30 min at RT, rinsed once in PBS and mounted on a glass slide using ProLong Gold® antifade reagent (Life Technologies). The slides were kept in dark overnight and confocal images were obtained using a Zeiss Stallion Dual Detector Imaging System with Intelligent Imaging Innovations Software (Carl Zeiss, Thornwood, NY).

Ovaries were labeled with primary antibodies for VASA (germ-cell marker) and GATA-4 (somatic cell marker), and imaged with a Zeiss 510 Meta multiphoton/confocal microscope (Carl Zeiss). For each ovary, two cores were visualized and counted. A core is a region 135 × 135 μm^2 consisting of optical sections at four different depths in the ovary, each 15–20 μm apart. Thus, for each ovary, two cores were obtained consisting of four optical sections per core for a total of eight optical sections per ovary. The number of germ cells found in the cyst relative to the total number of oocytes was determined for each ovary by analyzing each section and reported as percent single oocytes. In order to determine whether oocytes were in cysts or not, for each of the four optical sections in a core, a z-stack of images each 1 μm apart was obtained with five images above the section and five images below the section being analyzed. This allowed us to determine whether an oocyte was part of a GCC above or below the plane of focus. Follicle development was determined by counting the number of primordial and primary follicles present in relation to the total number of follicles found and reported as percent primordial and primary follicles.

Immunohistochemistry

Ovaries were fixed in 4% buffered paraformaldehyde (PFA) (6 g PFA, 325 mg NaOH, and 15 ml 10× PBS in 100 ml diethylpyrocarbonate-treated double distilled H_2O, pH 7.2) for 1 h at 4 °C and processed using standard procedures (Kerr et al., 2006). Paraffin sections (5 μm) were used for immunohistochemical (IHC) localization of proteins using a Vectastain Elite ABC kit (Vector Labs, Burlingame, CA) as previously described (Lee et al., 2012a; Lee et al., 2012b) and according to the manufacturer's protocols. The tissue sections were incubated with primary antibodies for p-AKT, p-ERK, p53, p27, SOD-2, caspase-3, BAX and X-linked Inhibitor of Apoptosis Protein (XIAP) at specific concentrations (as indicated in Table 1). The sections were further incubated with the secondary antibody (biotinylated IgG) for 45 min at RT. Negative controls included serum or IgG from the appropriate species related to the primary antibody at the same dilution. Digital images were captured using a Zeiss Axioplan 2 research microscope with an Axiocam HR digital camera (Carl Zeiss). The intensity of staining for each protein was quantified using Image-pro Plus as described previously (Lee et al., 2012a; Lee et al., 2012b) according to the manufacturer's instructions (Media Cybernetics, Inc., Bethesda, MD).

Antibodies

Sources of antibodies, catalog numbers, dilution, host species, immunogen and homology with rat/mouse are given in Table 1

Table 1
Primary and secondary antibodies, company, calalog number, dilution, immunogen, percentages of homology with rat and mouse, dilution and application.

Antibody	Company & Cat #	Dilution	Host species	Immunogen	% of homology with rat/mouse	Secondary antibody	Dilution	Application
p-AKT	Cell signaling; 3787	1:50	Rabbit monoclonal	Mouse	Rat-100%; Mouse-100%	Goat anti-rabbit	1:200	IHC
p-AKT	Antibodies online; 349614	1:500	Mouse monoclonal	Human	Rat-100%; Mouse-100%	Goat anti-mouse alexa 594 red	1:200	Whole mount
p-ERK	Cell signaling; 4370	1:100	Rabbit monoclonal	Human	Rat-100%; Mouse-100%	Goat anti-rabbit	1:200	IHC
p53	AbCam; 131442	1:200	Rabbit polyclonal	Human	Rat-100%; Mouse-100%	Goat anti-rabbit alexa 488 green	1:200	Whole mount
p53	Cell signaling; 2524	1:500	Mouse monoclonal	Human	Rat-93%; Mouse-93%	Goat anti-mouse alexa 488 green	1:200	Immuno-colocalization
SOD-2	Sigma; S1450	2 μg/ml	Rabbit polyclonal	Human	Rat-94%; Mouse-88%	Goat anti-rabbit	1:200	IHC
Caspase-3	Cell signaling; 9661	1:50	Rabbit polyclonal	Human	Rat-100%; Mouse-100%	Goat anti-rabbit	1:200	IHC
BAX	Sigma; SAB 4502549	1:1000	Rabbit polyclonal	Human	Rat-93%; Mouse-94%	Goat anti-rabbit	1:200	IHC
BAX	Cell signaling; 2774	1:50	Rabbit monoclonal	Human	Rat-76%; Mouse-76%	Goat anti-rabbit	1:200	IHC
XIAP	Cell signaling; 2045	1:100	Rabbit monoclonal	Human	Rat-82%; Mouse-82%	Goat anti-rabbit	1:200	IHC
p27	Cell signaling; 2552	1:500	Rabbit polyclonal	Mouse	Rat-100%; Mouse-100%	Goat anti-rabbit	1:200	IHC
VASA	Abcam; 13840	1:100	Rabbit polyclonal	Human	Rat-95%; Mouse-98%	Goat Anti-rabbit	1:200	IHC
GATA-4	Santa Cruz; 1237	1:100	Goat polyclonal	Mouse	Rat-100%; Mouse-100%	Rabbit anti-goat	1:200	IHC
GATA-4	Santa Cruz; 25310	1:50	Mouse monoclonal	Human	Rat-75%; Mouse-77%	Goat anti-mouse alexa 594 red	1:200	Whole mount

Analysis of oocyte numbers

Oocyte numbers were determined by counting the number of germ cells positive for VASA found within each optical section used for analyzing GCC breakdown and follicle development. The numbers were averaged and reported as number of oocytes per section.

Statistical analysis

Effects of CrVI on various parameters in the ovary were analyzed and the results were expressed as mean ± SEM. Student *t*-test was used to compare groups and *p* values less than 0.05 were considered significant. Pearson's correlation was used to derive '*R*' values for colocalization of p53 and SOD-2 between control and treatment groups.

Results

Gestational exposure to CrVI increased Cr levels in the placenta

Almost all tissues accumulate chromium (Collins et al., 2010). In order to determine if Cr passes through the placenta, we determined Cr levels in the placenta on gestational day 20. Rats were given CrVI through drinking water in order to mimic human exposure to CrVI. Gestational exposure to CrVI significantly elevated total Cr levels in the placenta (Fig. 1A).

CrVI induced early reproductive senescence

Our previous studies indicated that Cr exposure through lactation increases follicular atresia. In order to determine if *in utero* exposure to Cr induces reproductive failure in F1 offspring, we studied pregnancy rates, live births and litter size in Cr-exposed F1 females for a period of 10 months. Results show that *in utero* exposure to CrVI decreases pregnancy rate (Fig. 1B) and litter size (Fig. 1C) in F1 offspring up to 10 months. At the end of 10 months of age, only 2% of rats became pregnant in the CrVI-treatment group. It is evident that prenatal exposure to CrVI decreases pregnancy outcome and reduces litter size throughout age (Fig. 1B and C).

CrVI accelerated oocytes/germ cells and somatic/granulosa cells apoptosis and advanced primordial follicle assembly and primary follicle transition

The number of primordial follicles within the ovary determines the life-time follicle reserve. Even though successful assembly of the primordial follicle is one of the most critical events and the first step in folliculogenesis, proper timing of primordial follicle assembly is strictly regulated. The timing of folliculogenesis varies from species to species; however, both genesis and survival of primordial follicles determine the reproductive life of a female. Effects of CrVI on death of germ cells and primordial follicle assembly were determined. PND-1 control ovaries (Fig. 2A, C and E) consisted of intact and healthy oocytes arranged in the cysts. Ovigerous cords were readily observed and pyknotic nuclei of germ cells and somatic cells were infrequently observed. In contrast, CrVI induces germ cell cyst breakdown and primordial follicle assembly (Fig. 2B, D and F). Further, > 65% of the ovaries contained numerous primordial follicles whereas ovigerous cords were rarely observed and often disrupted (Fig. 2G). CrVI also significantly increased TUNEL-positive germ cells and somatic cells (Fig. 2H), compared to control.

CrVI advanced germ cell cyst breakdown

In mice, GCC breakdown begins in the medulla approximately at 17.5 days post-coitum (DPC) and in the cortex at 19.5 DPC, peaks at PND-2 and -3, and continues up to PND-4 with a concomitant loss of oocytes (Pepling and Spradling, 2001a). Effects of CrVI on germ cell cyst breakdown were determined by co-immunolocalization of VASA (germ cell marker) and GATA-4 (somatic cell marker) in whole mount ovaries. PND-1 control ovaries (Fig. 3A, C and E) consisted of intact and healthy germ cells arranged as groups of 10–24 healthy round oocytes inside the cysts with no detectable primordial follicles; whereas, few cysts and mostly primordial and primary follicles or small groups of irregularly shaped oocytes were present in CrVI treated animals indicative of advanced germ cell cyst breakdown (Fig. 3B, D and F). CrVI also

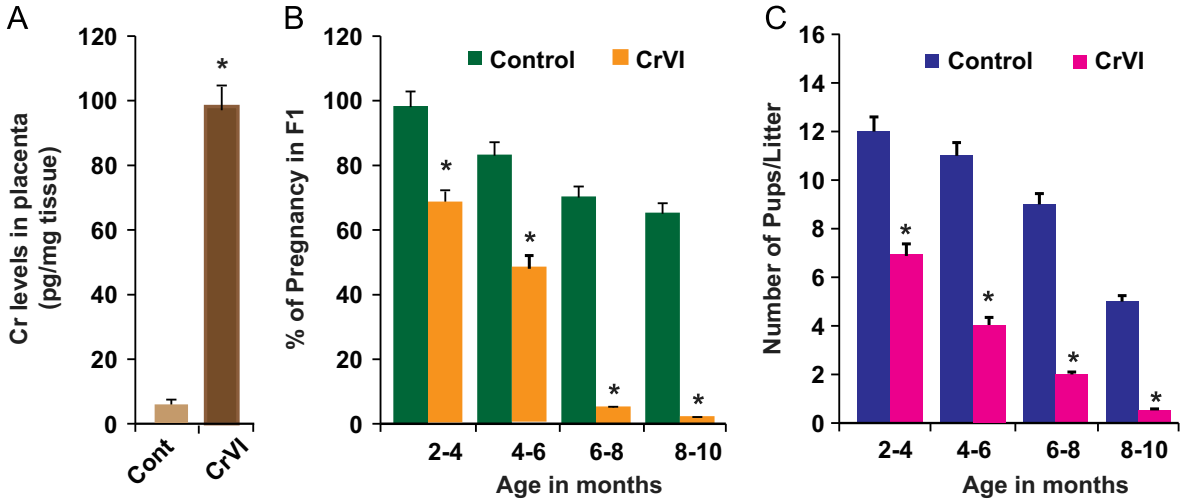

Fig. 1. Prenatal exposure to CrVI increases Cr accumulation in the placenta (A), and decreases pregnancy rate (B), and litter size (C) in the F1 female offspring. Pregnant mother rats (F0) received either regular drinking water (control) or CrVI (potassium dichromate 25 ppm) in drinking water from 9.5to 14.5 days postcoitum (DPC). Developing fetuses (F1) received CrVI through placental transfer from gestational days (GD) 9.5 to 14.5. On the GD 20, one group ($n=5$) of control and experimental mothers is euthanized and the placentae are removed. Total Cr is estimated in the placenta. Another set of control and CrVI-treated F1 females is allowed to breed for a period of 12 months ($n=15$). Numbers of rats that attained pregnancy (% pregnancies) (B) and delivered live pups are recorded every month. The number of pups/litter (litter size) (C) is recorded. *: control vs CrVI, $p<0.05$. Each value represents mean ± SEM of 20 F1 rats during a period of 2 months.

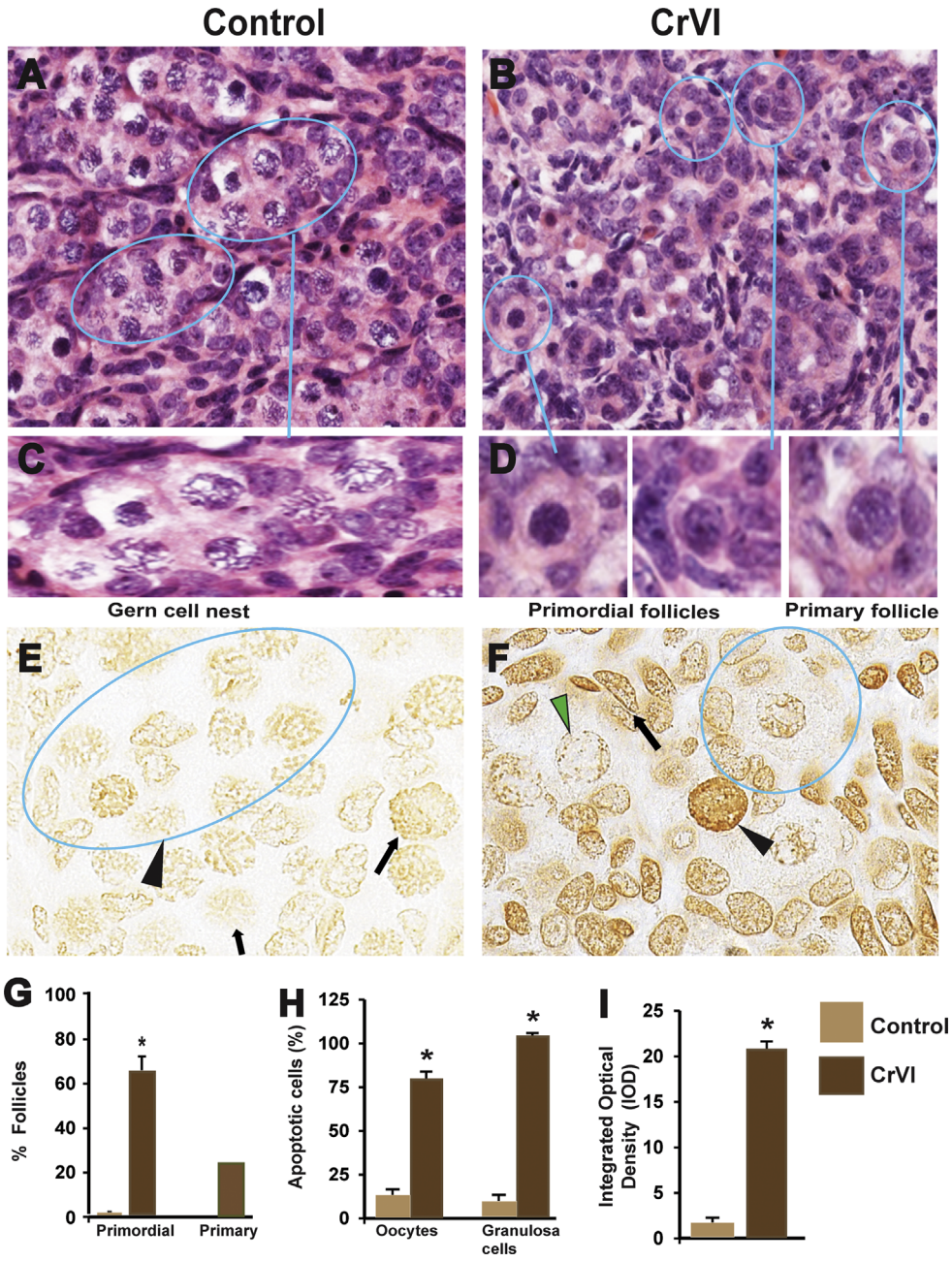

Fig. 2. Prenatal exposure to CrVI advanced primordial follicle assembly (B, D and G) compared to control (A, C and G). CrVI increased apoptosis of germ cells and somatic cells (E, F and H) in the F1 female offspring. Pregnant mother rats (F0) ($n=5$) received either regular drinking water (control) or CrVI (potassium dichromate 25 ppm) ($n=5$) in drinking water from GD 9.5 to 14.5. On postnatal day (PND)-1, F1 female pups are euthanized and the ovaries are removed and processed for histology (H and E), or TUNEL assay. Total number of primordial follicles is counted in every 10th section of the ovary. Integrated Optical Density (IOD) of the TUNEL-positive cells is quantified by Image ProPlus software. *: control vs CrVI, $p < 0.05$. Each representative image is magnified to 400 × (A and B). Each value represents mean ± SEM of 10–15 ovaries of the F1 pups. Insets in C and D are enlarged images of the area within the blue circles. In Fig. 2E, arrows indicate germ cells/oocytes, and arrowhead indicates germ cell cyst. In Fig. 2F, green arrow head indicates healthy oocyte, black arrow head indicates apoptotic oocyte, arrow indicates apoptotic granulosa cell and circle indicates primordial follicle.

decreased the number of intact oocytes per section (Fig. 3G), and increased the number of single oocytes (Fig. 3H).

CrVI down regulated cell survival proteins p-AKT, p-ERK1/2 and XIAP and up-regulated BAX and caspase-3

p-AKT, p-ERK1/2 and XIAP are abundantly expressed in control ovaries. Prenatal exposure to CrVI down-regulated the expression of p-AKT, p-ERK and XIAP proteins in the PND-1 ovaries of F1 pups (Fig. 4 A–I). It is well established that the size of the primordial follicle pool is regulated by BAX (Greenfeld et al., 2007b; Perez et al., 1999a) and BAX is a marker protein for POF (Matikainen et al., 2001). PND-1 ovaries of control F1 pups indicated that BAX and caspase-3 levels were very low whereas prenatal exposure to CrVI exhibited increased expression of BAX and caspase-3 compared to control (Fig. 5A–F).

CrVI up-regulated p53, SOD-2 and p27

p53 is a tumor suppressor, and our previous findings indicated that lactational exposure to CrVI increased granulosa cell apoptosis through a p53-mediated pathway (Banu et al., 2011). However, there are no data available on the role of p53 in GCC breakdown under normal conditions or in response to any toxicant. p27 is

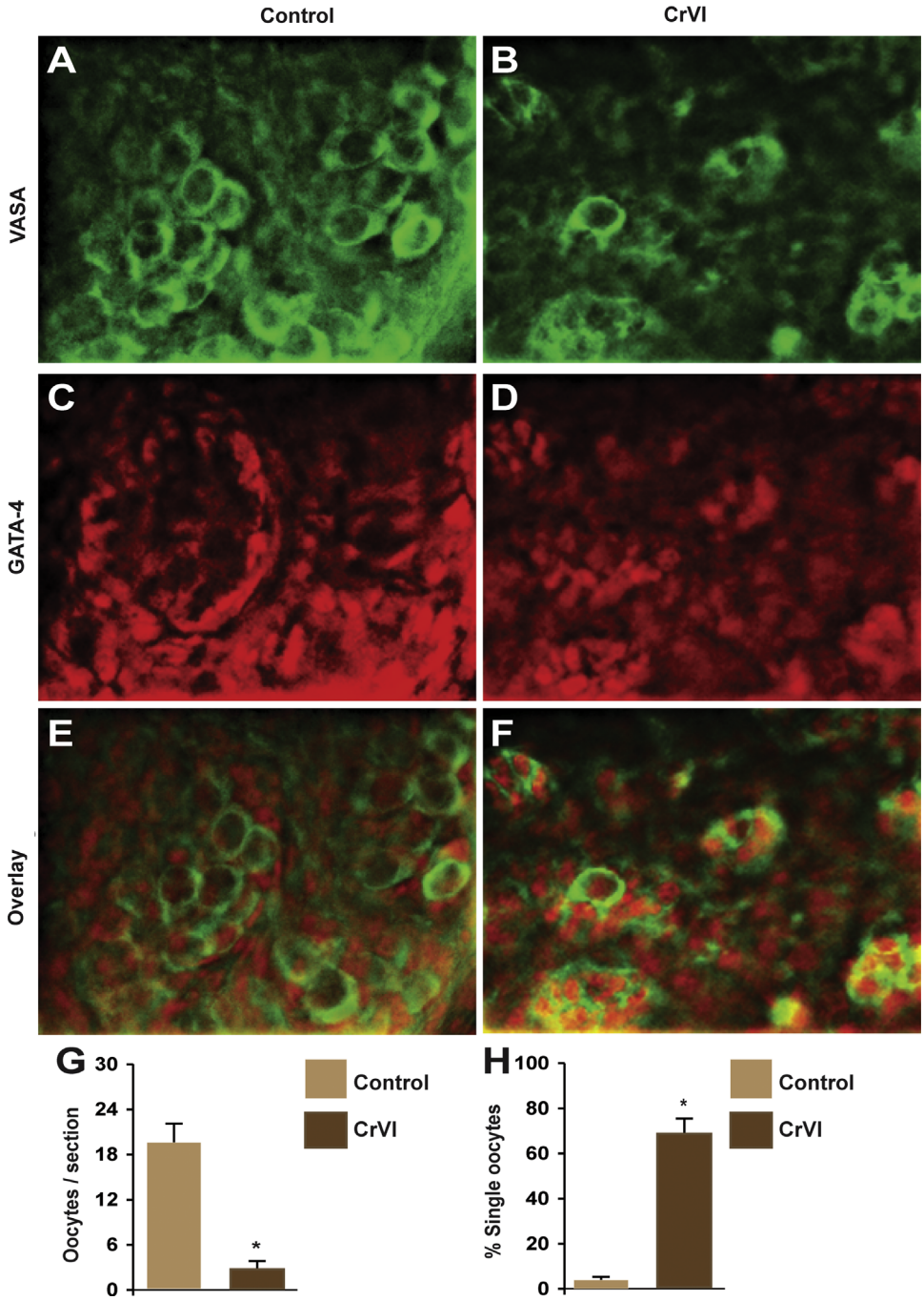

Fig. 3. Prenatal exposure to CrVI accelerated germ cell cyst (GCC) breakdown and advanced primordial follicle assembly and primary follicle transition. On PND-1, ovaries from F1 female pups are processed for whole mount double immunofluorescence assay or histology. Germ cells are identified by germ cell marker VASA (green, A and B), and somatic cells by somatic cell marker GATA-4 (red, C and D), with overlay shown in E and F. Number of germ cells or oocytes per section (G) and percentage of single oocytes (H) are shown. Every 10th section of the paraffin-embedded ovary is stained with H and E for counting primordial and primary follicles. *: control vs CrVI, $p < 0.05$. Each value represents mean ± SEM of 10–15 ovaries of the F1 pups.

also a tumor suppressor and negative regulator of cell cycle progression, activated caspase-3, and follicular atresia (Rajareddy et al., 2007), and plays a crucial role in fetal ovary development (Nagahama et al., 2001; Rajareddy et al., 2007). In order to determine the expression of p53 and p27 in GCC breakdown, both proteins were analyzed by IHC. p53 expression in control PND-1 ovaries was non-detectable whereas gestational exposure to CrVI increased p53 protein expression (Fig. 6A, B and G). CrVI also increased p27 expression compared to control. In both control and CrVI-treated ovaries, p27 was localized in the somatic cells rather than the germ cells (Fig. 6C, D and H). Previous findings indicate that p53 reduces SOD-2 activity (Zhao et al., 2005). SOD-2 is expressed in the oocytes of the dormant primordial follicles (El Mouatassim et al., 1999). A low level of SOD-2 was detectable in control oocytes (Fig. 6E, F and I), and CrVI significantly increased SOD-2 (Fig. 6E, F and I).

CrVI increased co-localization of p53 and SOD-2 in whole mount ovaries

IHC showed increased expression of p53 and SOD-2 in CrVI-treated rats (Fig. 6). SOD-2 is often times associated with granulosa

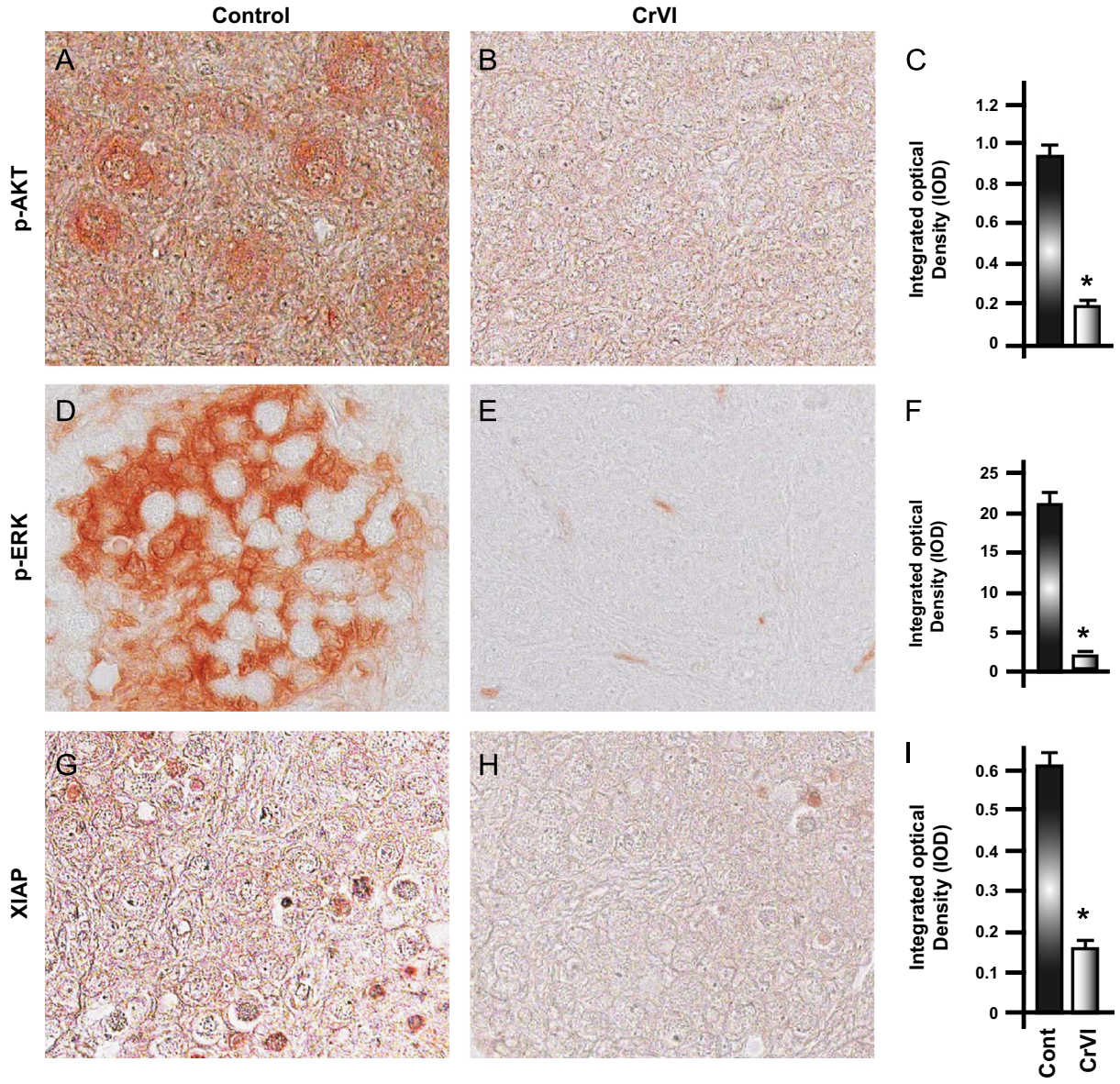

Fig. 4. Prenatal exposure to CrVI down regulated the expression of p-AKT, p-ERK and XIAP proteins in the PND-1 ovaries of the F1 pups. On PND-1, ovaries from F1 female pups are processed for immunohistochemistry. Integrated Optical Density (IOD) is quantified by Image ProPlus software. Each representative image is magnified to 400 ×; p-AKT (A–C), p-ERK (D–F), and XIAP (G–I). *: control vs CrVI, $p < 0.05$. Each value represents mean ± SEM of 10–15 ovaries of the F1 pups.

cell (Stanley et al., 2013) and primordial follicle survival (Matzuk et al., 1998), as a protective mechanism to prevent oxidative stress (Matzuk et al., 1998). Therefore, we monitored co-localization of SOD-2 and p53, by evaluating the levels of expression and co-localization of both the proteins in the PND-1 ovaries. In control PND-1 ovaries, p53 expression was non-detectable (Fig. 7A and D); and SOD-2was abundantly expressed (Fig. 7 B and E). Interestingly, CrVI increased the expression levels of both p53 (Fig. 7 G and J), and SOD-2 (Fig. 7H and K). CrVI significantly increased p53–SOD-2 co-localization compared to control (Fig. 7C, F, I, L and M–P).

Discussion

The main goal of this study was to determine the role of CrVI in causing early reproductive senescence and to explore the underlying molecular mechanism. Our earlier studies documented that postnatal exposure to Cr through mother's milk increased follicle atresia and delayed pubertal onset (Banu et al., 2008; Stanley et al., 2013), although effect of Cr on fertility outcome of the F1 females is not known. The present study indicates that *in utero* exposure to CrVI increases Cr levels in the placenta and causes early reproductive senescence leading to a significant reduction in litter size in the F1 generation. This is consistent with the previous studies indicating that endocrine disruptors can adversely affect the follicular reserve and reproductive longevity in the female species (Gregoraszczuk and Ptak, 2013), even though the mechanisms are not known. Therefore, we examined the key molecular mechanism behind the gestational exposure to CrVI on female reproductive failure in the F1 offspring.

Follicular development begins *in utero* with the transformation of primordial germ cells into oocytes (Hirshfield, 1997) that comprises various steps from the breaking down of GCC to the development of pre-ovulatory follicles. In most mammals, primordial follicles form either before or during the first few days after birth (Hirshfield, 1997; Hirshfield and DeSanti, 1995). One-third of the primordial follicles undergo rapid atresia within few days after birth. The ultimate surviving number of primordial follicles

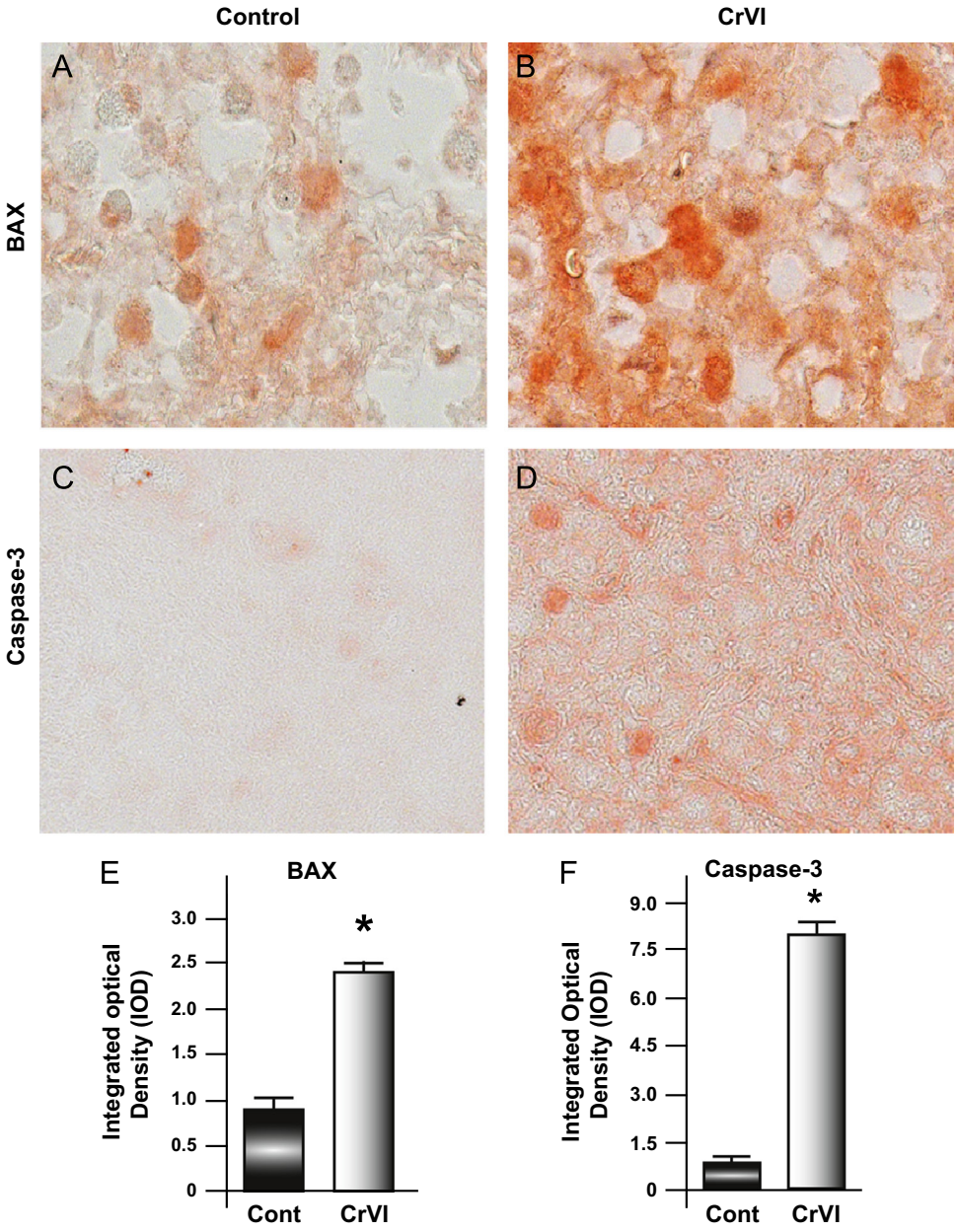

Fig. 5. Prenatal exposure to CrVI up-regulated the expression of BAX and cleaved-caspase-3 proteins in the PND-1 ovaries of the F1 pups. On PND-1, ovaries from F1 female pups are processed for immunohistochemistry. Integrated Optical Density (IOD) is quantified by Image ProPlus software. Each representative image is magnified to 400X; BAX (A, B, E) and cleaved caspase-3 (C, D, F). *: control vs CrVI, $p < 0.05$. Each value represents mean $\pm$ SEM of 10–15 ovaries of the F1 pups.

determines the lifetime follicle reserve (Hirshfield, 1994). Defects in either the timing or process of GCC breakdown can result in improper primordial follicle assembly and/or accelerated atresia, resulting in early reproductive senescence or infertility. In mice, GCC breakdown typically starts from gestational day 17.5 (Pepling et al., 2010), reaching the maximum between PND-2 and -3 (Pepling and Spradling, 2001b). In control rats, primordial follicles started to appear on PND-4 (Gelety and Magoffin, 1997; Jones, 2012). However, exact developmental milestones of GCC breakdown, germ cell death and primordial follicle assembly are not precisely detected in rats. For the current study, we chose PND1 to identify the mechanism through which gestational exposure to CrVI disrupts the early development of the ovary.

Interestingly, our data revealed that CrVI increased germ cell death, accelerated GCC breakdown, advanced primordial follicle assembly and transition to primary follicles. On PND-1, control ovaries appeared to have very well organized ovigerous cords with 10–24 germ cells/oocytes in the GCC. In the mammalian ovary, the proliferating oogonia or germ cells in association with somatic cells are partitioned into irregularly shaped ovigerous cords radially oriented towards and open to the surface of the ovary. Later in development, commencing at the base of the cords, the somatic cells closely associate with oogonia and together develop into primordial follicles. In rats, primordial follicles form between PND-3 and -4. However in CrVI-treated rats, there were several follicles with oocytes encapsulated by either flat and/or cuboidal granulosa cells on PND-1. Thus, most of the follicles are at the primordial stage or early primary stage. According to the early studies on rats, primordial follicles are formed on the PND-4 (Gelety and Magoffin, 1997; Jones, 2012; Pepling, 2012a). Our data showed a striking difference in that CrVI exposure advances follicle assembly and transition of primordial to primary follicles, the ovaries had greater numbers of primordial as well as primary follicles on PND-1. Moreover, most of these follicles were in the

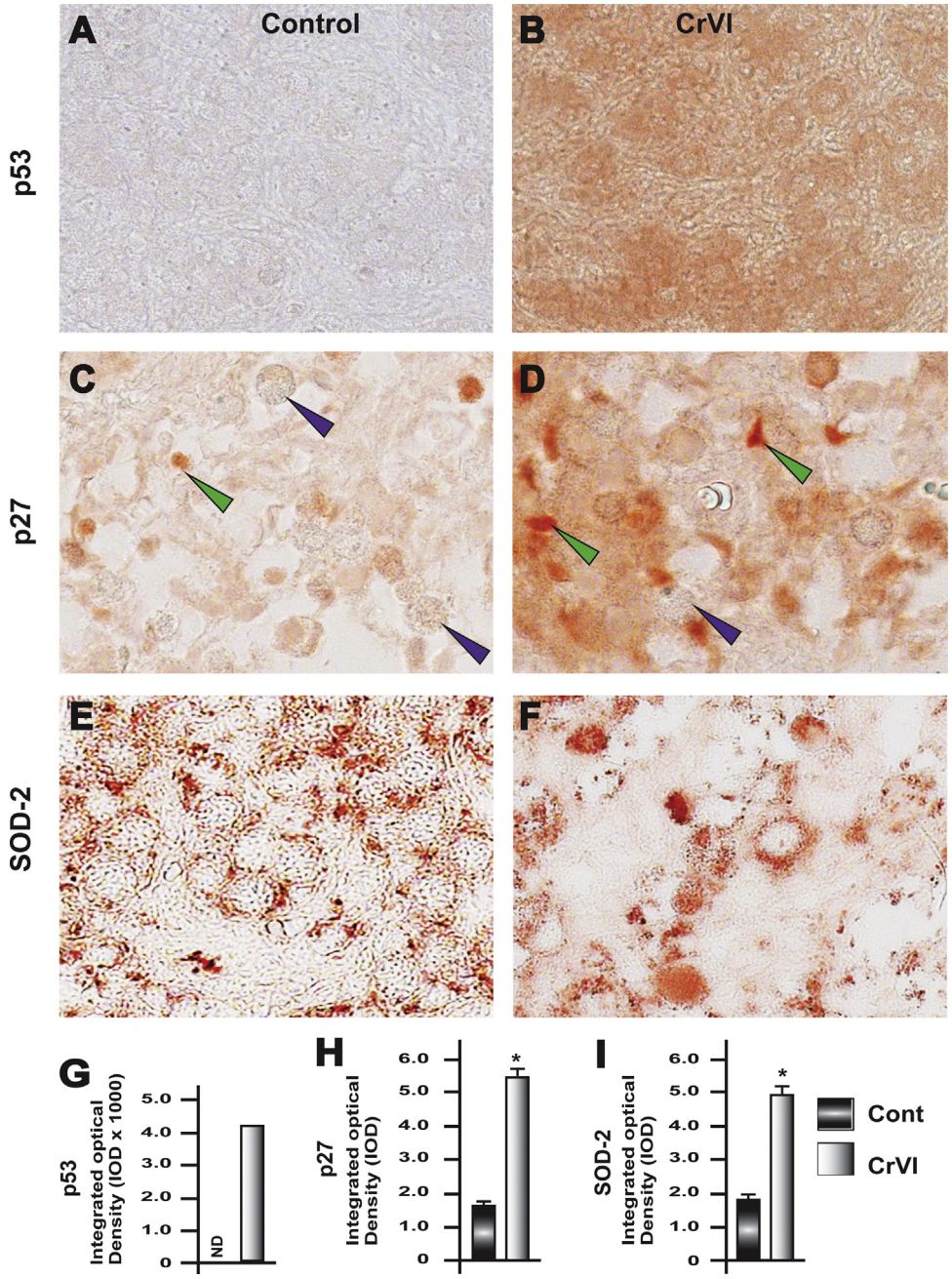

Fig. 6. Prenatal exposure to CrVI up-regulated the expression of p53, p27 and SOD-2 proteins in the PND-1 ovaries of the F1 pups. On PND-1, ovaries from F1 female pups are processed for immunohistochemistry. Integrated Optical Density (IOD) is quantified by Image ProPlus software. Each representative image is magnified to 400 × ; p53 (A, B and G), p27 (C, D and H), and SOD-2 (E, F, and I). Green arrow heads indicate somatic cells, and purple arrow heads indicate germ cells or oocytes. *: control vs CrVI, $p < 0.05$. Each value represents mean ± SEM of 10–15 ovaries of the F1 pups.

process of atresia. Follicle loss takes place either from the initial follicle pool by atresia, or merely by the healthy transition to the next phase of follicular growth (Tingen et al., 2009b). Thus our data for the first time documented that gestational exposure to CrVI caused early follicle senescence through increased germ cell death, accelerated GCC breakdown, advanced primordial follicle assembly and primary follicle transition. However, the mechanism that facilitates the extensive germ cell death during the perinatal period in mammalian species is not well understood. There are no data available on the effect of CrVI on the germ cell death and GCC breakdown. Therefore, in order to identify the underlying mechanism, we studied the expression, regulation and interactions of the key cell survival and apoptotic regulatory proteins in the ovary of CrVI-exposed F1 offspring on PND-1.

The PI3K/AKT signaling pathway is a well-known critical regulatory network that governs follicle growth, differentiation and survival among the several regulatory pathways controlling oogenesis (Canipari et al., 2012; Cecconi et al., 2012; Cecconi et al., 2010; Edson et al., 2009). Deletion of AKT causes infertility and POF indicating its essential role in preserving the normal female reproductive lifespan (Edson et al., 2009). Moreover, the function of growth factor-mediated MAPK signaling is largely unknown in the early development of the ovary. Our results indicate that ovaries from control rats abundantly expressed p-AKT and p-ERK on PND-1, which is critical for germ cell survival and growth. CrVI decreased p-AKT and p-ERK compared to control. This suggests that CrVI may have partly induced germ cell death and accelerated GCC breakdown by decreasing p-AKT and p-ERK. XIAP is a pro-

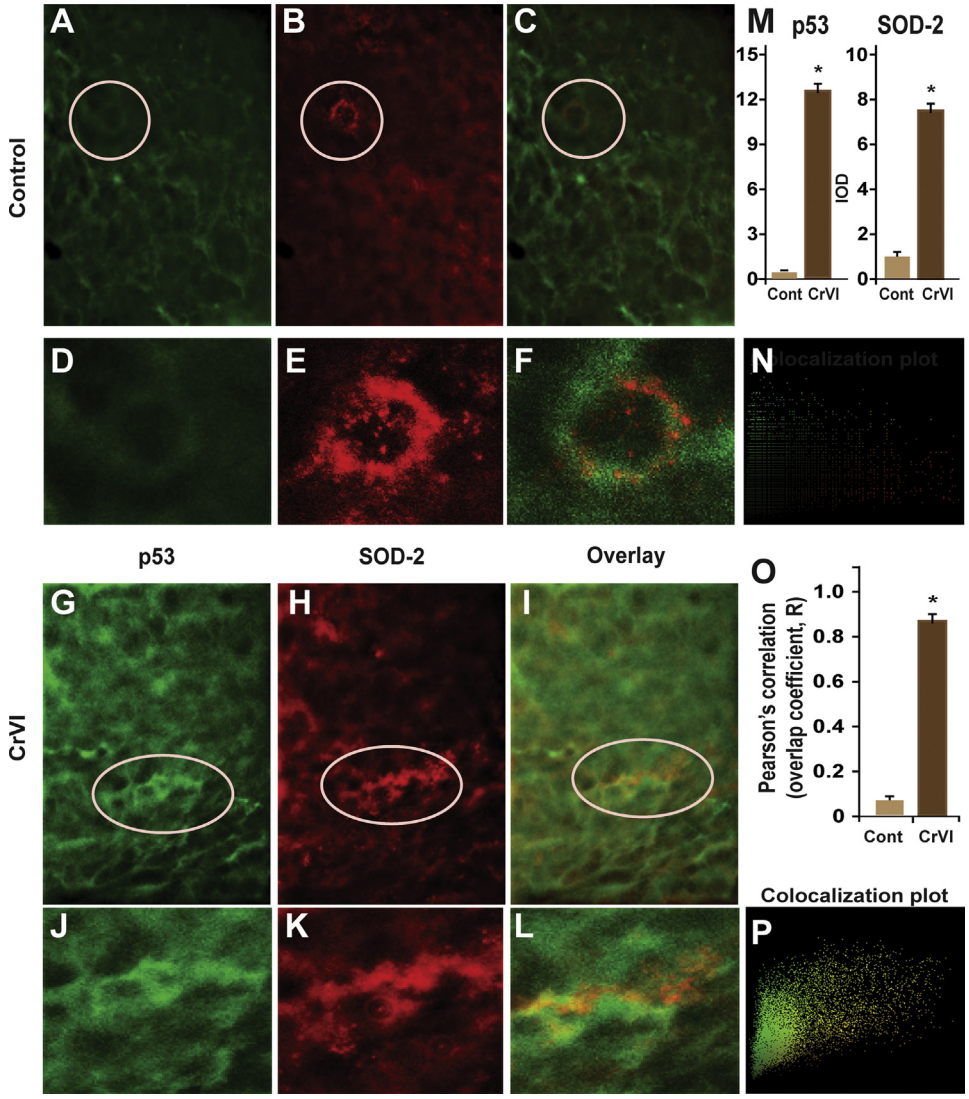

Fig. 7. Prenatal exposure to CrVI increased co-localization of p53 and SOD-2 proteins in the PND-1 ovaries of the F1 pups. On PND-1, ovaries from F1 female pups are processed for whole mount double immunofluorescence. Co-localization of p53 and SOD-2 proteins is measured by co-localization index of the p53 and SOD-2; and the degree of co-localization is measured by the "color composite" and "co-localization" functions in Image-ProPlus software. In control group, p53 expression is very minimal (green, A and D); and SOD-2 is abundantly expressed (red, Fig. 7 B and E). CrVI increases the expression levels of both p53 (G and J), and SOD-2 (H and K). CrVI significantly increases co-localization of p53 and SOD-2 proteins compared to control (overlay, C, F, I, L and M–P). The scatter plot displays the intensity range of red and green pixels in the image (N and P). Integrated Optical Density (IOD) is quantified by Image ProPlus software. *: control vs CrVI, $p < 0.05$. Each value represents mean ± SEM of 10–15 ovaries of the F1 pups.

survival protein, belonging to the family of inhibitors of apoptosis proteins (IAPs) that represent a conserved gene family whose translated products protect against apoptosis induced by a broad spectrum of death-inducing stimuli such as death receptor ligands, chemotherapeutic agents, pro-apoptotic members of the Bcl-2 family and cytochrome *c* release (Phillipps and Hurst, 2012). Our data showed that CrVI downregulated XIAP in PND-1 ovary. XIAP suppresses caspase-3 and caspase-7 activities (Ekert et al., 2001; Johnson and Bridgham, 2002). It is suggested that CrVI-induced down regulation of XIAP might have released caspases from the inhibitory effects of XIAP, and increased apoptosis of germ cells to enhance germ cell death and GCC breakdown.

BAX is a regulator of germ cell death that regulates the size of the primordial follicle pool (Felici et al., 1999; Greenfeld et al., 2007a). BAX is upregulated in the ovaries during germ cell atresia and in fetal germ cells undergoing apoptosis (Felici et al., 1999). BAX is involved in promoting the death of ectopic germ cells that fail to migrate correctly to the gonads (Stallock et al., 2003). BAX negatively regulates the primordial follicle pool by promoting germ cell atresia and GCC breakdown. Perez et al. demonstrated that $BAX^{-/-}$ females have prolonged reproductive longevity due to reduced atresia of immature follicles (Perez et al., 1999b). CrVI upregulates BAX expression in the PND-1 ovaries and induces POF. Based on the previous findings, our data suggest that CrVI-induced increase in BAX in the fetal ovaries may have contributed to the extensive germ cell apoptosis and accelerated GCC breakdown, resulting in POF. Interestingly, caspase-3 dependent apoptosis seems to be the most important, but not the only pathway of cell death in the human fetal ovary (Hussein, 2005; Poljicanin et al., 2013). During embryonic stages of human development a caspase-independent cell death pathway operates in the process of germ cell death, while during fetal development, a caspase-dependent pathway is a major cell death mechanism. In post-natal ovaries, caspase-dependent cell death begins in granulosa cells and not in the germ cells. Therefore, apoptosis in human ovaries appears to be a selective process that is executed by different cell death pathways in different ovarian cell populations, and is dependent on the stage or window of follicle development/atresia (Poljicanin

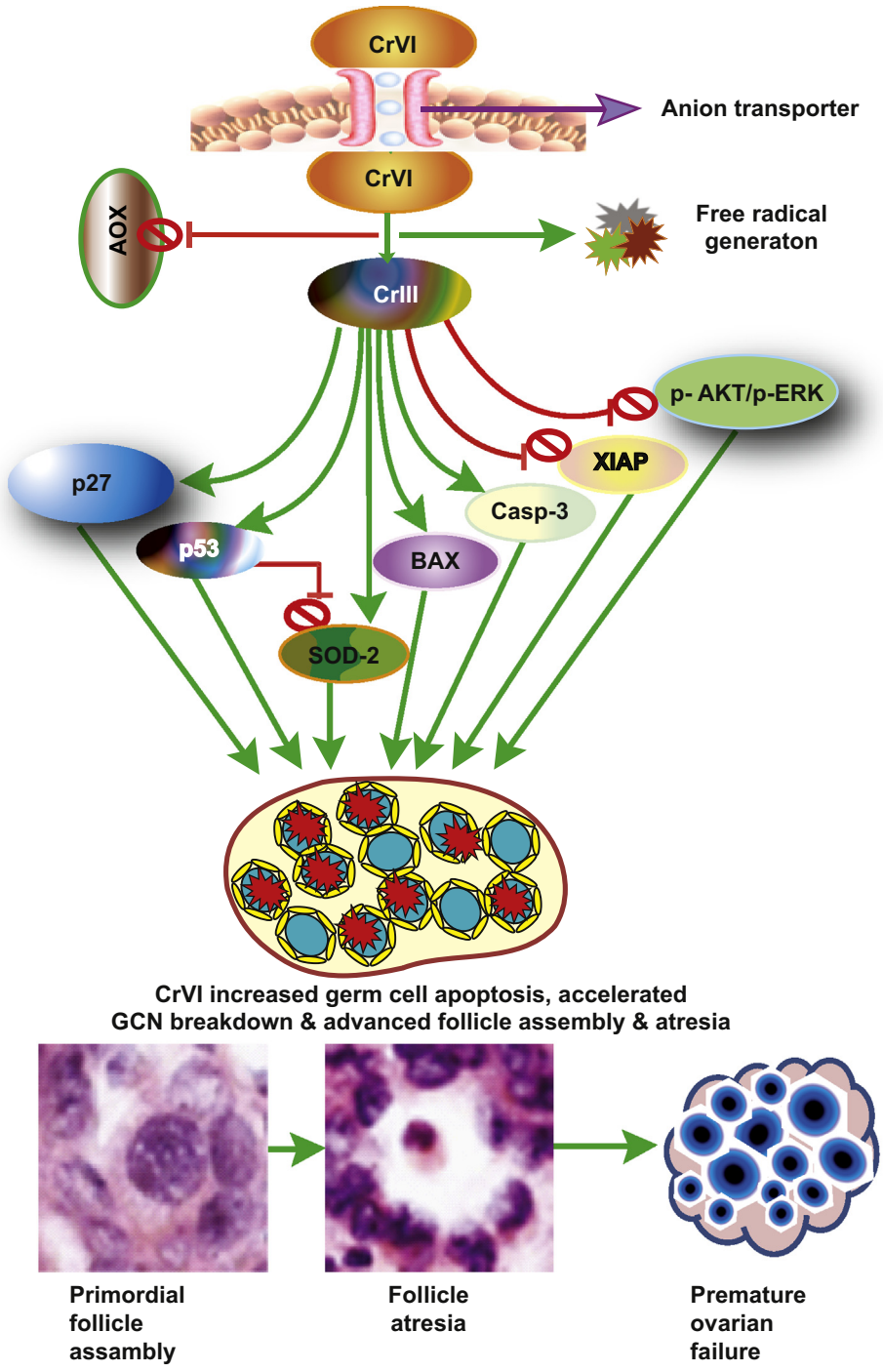

Fig. 8. Schematic diagram representing the involvement of key proteins in CrVI-induced ovotoxicity during fetal ovary development. Prenatal exposure to CrVI during GD 9.5–14.5, upregulates the expression of the pro-apoptotic p53, p27, BAX, and cleaved-caspase-3, along with SOD-2. CrVI increases co-localization of p53 and SOD-2 proteins, and p53 inhibits the antioxidant function of the SOD-2. CrVI also down regulates the expression of p-AKT, p-ERK,and XIAP, thus reduces the pro-survival pathways. As a result of these events, CrVI accelerates germ cell and somatic cell apoptosis, advances GCC breakdown, primordial follicle assembly, and enhances primordial to primary follicle transition, culminating in increased follicular atresia. All these adverse effects of CrVI ultimately resulted in early reproductive senescence/POF.

et al., 2013). Reports from the Woodruff's laboratory also endorse a similar phenomenon in the rodent ovary (Tingen et al., 2009a; Tingen et al., 2009b). Interestingly, our data indicates that caspase-3 is almost undetectable in control ovaries on PND-1, suggesting the possibility of the existence of caspase-3-independent mechanism during normal ovarian development and physiological germ cell death. Since CrVI significantly increases caspase-3 expression in the PND-1 ovary, we suggest that CrVI may have increased germ cell apoptosis and accelerated GCC breakdown through a caspase-3-mediated mechanism downstream of BAX. This study for the first time suggests that BAX and caspase-3 may be a part of the apoptotic orchestra in executing germ cell death in response to gestational exposure to CrVI.

Our previous finding indicated that p53 plays a critical role in CrVI-induced granulosa cell apoptosis (Banu et al., 2011). CrVI increased the expression, activation, stabilization and mitochondrial translocation of p53 in granulosa cells which precedes apoptosis (Banu et al., 2011). The role of p53 in the fetal ovarian

development has not been studied in any species. p53 protein is not detected in mouse ovaries during fetal days 13.5–18.5, even though it is expressed in fetal testes (Matsui et al., 2000). Interestingly, our data reveal that p53 is undetectable in control rat ovaries on PND-1. However, CrVI induced and up-regulated the expression of p53. p53 is known to bind with SOD-2 protein in the mitochondria in JB6 skin epidermal cells, and to suppress the antioxidant property of SOD-2 (Zhao et al., 2005). Interestingly, following p53 mitochondrial translocation and matrix localization, p53 interacted with SOD-2 that increased oxidative stress (Zhao et al., 2005). Two-color immunofluorescence on whole mount ovaries on PND-1 revealed that CrVI upregulated SOD-2, and increased the co-localization of p53 and SOD-2. CrVI not only increased the expression of p53 but also enhanced its translocation into mitochondria to inhibit SOD-2 reactive oxygen species scavenging and thereby executed apoptosis of germ cells and early GCC breakdown.

Our data revealed that p27 was predominantly expressed in the somatic cells rather than in the germ cells/oocytes of the PND-1 ovary. Rajareddy et al. (Rajareddy et al., 2007) had reported a similar finding where p27 was expressed in the somatic cells but not in oocytes of the mouse at embryonic day 14.5 and PND-1. p27 is a negative regulator of cell cycle progression and is a tumor suppressor (Kaldis, 2007). Interestingly, p27 activates the caspase-9–caspase-3–caspase-7–PARP apoptotic cascade by inhibiting Cdk2/Cdc2-cyclin A/B1 kinase activities in follicles, thereby inducing follicle atresia in the mouse (Rajareddy et al., 2007). Strikingly, the expression pattern of p27 (Fig. 6C and D) and TUNEL-labeling (Fig. 2E and F) in the somatic cells showed a close similarity. Our data suggests that CrVI may increase apoptosis of the somatic cells by upregulating p27 and disrupting somatic cell–germ cell paracrine interactions, and thereby contributing an additional mechanism for the germ cell apoptosis.

Taken together, as given in our working model (Fig. 8), CrVI is rapidly transported into the cells and reduced to CrIII. During this reduction process, a large amount of reactive oxygen species is generated, which increases oxidative stress and depletes antioxidants. In turn, CrIII either dephosphorylates or reduces the phosphorylation of p-AKT and p-ERK, decreases XIAP and thus inhibits cell survival machinery. CrIII up-regulates caspase-3 and BAX which leads to increased apoptosis of germ cells. CrIII also increases the expression and activation of p53 and facilitates the mitochondrial transport of p53. p53 interacts with SOD-2 and arrests its scavenging of reactive oxygen species which, in turn, augments the apoptotic response in germ cells. As a result of these molecular events, the large majority of the germ cells undergo apoptosis, or prematurely assemble into primordial follicles and transit into primary follicles, thus reducing the primordial follicle pool. In conclusion, these studies indicate that CrVI causes early reproductive senescence by (i) accelerating germ cell apoptosis through the p53/p27–BAX–caspase-3 pathway; (ii) advancing GCC breakdown and primordial follicle assembly; (iii) increasing primordial follicle transition into primary follicles; (iv) increasing follicular atresia; and (v) depleting the healthy primordial follicle pool resulting in a reduced follicular reserve.

Ongoing and future studies in our lab will explore the molecular mechanisms underlying these events during the critical phases of the fetal ovary development. In addition, intervention strategies to protect the ovary from the adverse effects of CrVI are under investigation.

Acknowledgments

This work was supported by National Institute of Environmental Health Sciences (NIEHS) Grant ES020561-01 to S.K.B.

References

Banu, S.K., 2013. Heavy metals and the ovary. In: Hoyer, P.B. (Ed.), Ovarian Toxicology, second ed. CRC Press/Taylor & Francis Group, Boca Raton, FL, pp. 193–229
Banu, S.K., Lee, J., Speights, V.O.J., Starzinski-Powitz, A., Arosh, J.A., 2009. Selective inhibition of prostaglandin E2 receptors EP2 and EP4 induces apoptosis of human endometriotic cells through suppression of ERK1/2, AKT, NFkappaB, and beta-catenin pathways and activation of intrinsic apoptotic mechanisms. Mol. Endocrinol. 23, 1291–1305.
Banu, S.K., Samuel, J.B., Arosh, J.A., Burghardt, R.C., Aruldhas, M.M., 2008. Lactational exposure to hexavalent chromium delays puberty by impairing ovarian development, steroidogenesis and pituitary hormone synthesis in developing Wistar rats. Toxicol. Appl. Pharmacol. 232, 180–189.
Banu, S.K., Stanley, J.A., Lee, J., Stephen, S.D., Arosh, J.A., Hoyer, P.B., Burghardt, R.C., 2011. Hexavalent chromium-induced apoptosis of granulosa cells involves selective sub-cellular translocation of Bcl-2 members, ERK1/2 and p53. Toxicol. Appl. Pharmacol. 251, 253–266.
Barceloux, D.G., 1999. Chromium. Clin. Toxicol. 37, 173–194.
Canipari, R., Cellini, V., Cecconi, S., 2012. The ovary feels fine when paracrine and autocrine networks cooperate with gonadotropins in the regulation of folliculogenesis. Curr. Pharm. Des. 18, 245–255.
Cecconi, S., Mauro, A., Cellini, V., Patacchiola, F., 2012. The role of Akt signalling in the mammalian ovary. Int. J. Dev. Biol. 56, 809–817.
Cecconi, S., Rossi, G., Santilli, A., Stefano, L.D., Hoshino, Y., Sato, E., Palmerini, M.G., Macchiarelli, G., 2010. Akt expression in mouse oocytes matured in vivo and in vitro. Reprod. Biomed. Online 20, 35–41.
Chen, Y., Jefferson, W.N., Newbold, R.R., Padilla-Banks, E., Pepling, M.E., 2007. Estradiol, progesterone, and genistein inhibit oocyte nest breakdown and primordial follicle assembly in the neonatal mouse ovary in vitro and in vivo. Endocrinology 148, 3580–3590.
Collins, B.J., Stout, M.D., Levine, K.E., Kissling, G.E., Melnick, R.L., Fennell, T.R., Walden, R., Abdo, K., Pritchard, J.B., Fernando, R.A., Burka, L.T., Hooth, M.J., 2010. Exposure to hexavalent chromium resulted in significantly higher tissue chromium burden compared with trivalent chromium following similar oral doses to male F344/N rats and female B6C3F1 mice. Toxicol. Sci. 118, 368–379.
De Felici, M., Lobascio, A.M., Klinger, F.G., 2008. Cell death in fetal oocytes: many players for multiple pathways. Autophagy, 4; , pp. 240–242.
Edson, M., Nagaraja, A., Matzuk, M., 2009. The mammalian ovary from genesis to revelation. Endocr. Rev. 30, 624–712.
Ekert, P.G., Silke, J., Hawkins, C.J., Verhagen, A.M., Vaux, D.L., 2001. DIABLO promotes apoptosis by removing MIHA/XIAP from processed caspase 9. J. Cell Biol. 152, 483–490.
El Mouatassim, S., Guerin, P., Menezo, Y., 1999. Expression of genes encoding antioxidant enzymes in human and mouse oocytes during the final stages of maturation. Mol. Hum. Reprod. 5, 720–725.
Felici, M.D., Carlo, A.D., Pesce, M., Iona, S., Farrace, M.G., Piacentini, M., 1999. Bcl-2 and Bax regulation of apoptosis in germ cells during prenatal oogenesis in the mouse embryo. Cell Death Differ. 6, 908–915.
Fenwick, M., Hurst, P., 2002. Immunohistochemical localization of active caspase-3 in the mouse ovary: growth and atresia of small follicles. Reproduction 124, 659–665.
Gelety, T.J., Magoffin, D.A., 1997. Ontogeny of steroidogenic enzyme gene expression in ovarian theca-interstitial cells in the rat: regulation by a paracrine theca-differentiating factor prior to achieving luteinizing hormone responsiveness. Biol. Reprod. 56, 938–945.
Giaccia, A.J., Kastan, M.B., 1998. The complexity of p53 modulation: emerging patterns from divergent signals. Genes Dev. 12, 2973–2983.
Greene, L.E., Riederer, A.M., Marcus, M., Lkhasuren, O., 2010. Associations of fertility and pregnancy outcomes with leather tannery work in Mongolia: a pilot study. Int. J. Occup. Environ. Health 16, 60–68.
Greenfeld, C.R., Babus, J.K., Furth, P.A., Marion, S., Hoyer, P.B., Flaws, J.A., 2007a. BAX is involved in regulating follicular growth, but is dispensable for follicle atresia in adult mouse ovaries. Reproduction 133, 107–116.
Greenfeld, C.R., Pepling, M.E., Babus, J.K., Furth, P.A., Flaws, J.A., 2007b. BAX regulates follicular endowment in mice. Reproduction 133, 865–876.
Gregoraszczuk, E.L., Ptak, A., 2013. Endocrine-disrupting chemicals: some actions of POPs on female reproduction. Int. J. Endocr. 2013, 9.
Haupt, S., Berger, M., Goldberg, Z., Haupt, Y., 2003a. Apoptosis – the p53 network. J. Cell Sci. 116, 4077–4085.
Haupt, S., Louria-Hayon, I., Haupt, Y., 2003b. P53 licensed to kill? Operating the assassin. J. Cell. Biochem. 88, 76–82.
Hawthorne, M., Toxic chromium found in Chicago drinking water, Chicago Tribune, Chicago, 2011.
Hirshfield, A.N., 1994. Relationship between the supply of primordial follicles and the onset of follicular growth in rats. Biol. Reprod. 50, 421–428.
Hirshfield, A.N., 1997. Overview of ovarian follicular development: considerations for the toxicologist. Environ. Mol. Mutagen. 29, 10–15.
Hirshfield, A.N., DeSanti, A.M., 1995. Patterns of ovarian cell proliferation in rats during the embryonic period and the first three weeks postpartum. Biol. Reprod. 53, 1208–1221.
Honeycutt, M.E., 2010. Hexavalent chromium in Texas drinking water. Toxicol. Sci. 119, 423–424.
Hussein, M.R., 2005. Apoptosis in the ovary: molecular mechanisms. Hum. Reprod. Update 11, 162–177.

Jefferson, W., Newbold, R., Padilla-Banks, E., Pepling, M., 2006. Neonatal genistein treatment alters ovarian differentiation in the mouse: inhibition of oocyte nest breakdown and increased oocyte survival. Biol. Reprod. 74, 161–168.
Jendryczko, A., Drozdz, M., Magner, K., 1984. Preliminary studies of chromium concentration in the myometrium in the third trimester of pregnancy, in chorionic tissue in the first trimester and in the blood of pregnant women. Ginekol. Pol. 55, 691–694.
Johnson, A.L., Bridgham, J.T., 2002. Caspase-mediated apoptosis in the vertebrate ovary. Reproduction 124, 19–27.
Johnson, A.L., Bridgham, J.T., Digby, M.R., Lowenthal, J.W., 1998. Expression of the inhibitor of T-cell apoptosis (ita) gene in hen ovarian follicles during development. Biol.Reprod. 58, 414–420.
Jones, R.L., Molecular Mechanisms Regulating Neonatal Oocyte Survival and Primordial Follicle Formation in the Mouse Ovary, Biology (Dissertation). Syracuse University, Syracuse, NY, 2012.
Kaldis, P., 2007. Another piece of the p27Kip1 puzzle. Cell 128, 241–244.
Kanojia, R.K., Junaid, M., Murthy, R.C., 1998. Embryo and fetotoxicity of hexavalent chromium: a long-term study. Toxicol. Lett. 95, 165–172.
Kerr, J.B., Duckett, R., Myers, M., Britt, K.L., Mladenovska, T., Findlay, J.K., 2006. Quantification of healthy follicles in the neonatal and adult mouse ovary: evidence for maintenance of primordial follicle supply. Reproduction 132, 95–109.
Layton, L., Probable carcinogen hexavalent chromium found in drinking water of 31 U.S. cities, The Washington Post, 2010.
Lee, J., Banu, S., Nithy, T., Stanley, J., Arosh, J., 2012a. Early pregnancy induced expression of prostaglandin E2 receptors EP2 and EP4 in the ovine endometrium and regulated by interferon tau through multiple cell signaling pathways. Mol.Cell. Endocrinol. 348, 211–223.
Lee, J., McCracken, J., Stanley, J., Nithy, T., Banu, S., Arosh, J., 2012b. Intraluteal prostaglandin biosynthesis and signaling are selectively directed towards PGF_{2alpha} during luteolysis but towards PGE_2 during the establishment of pregnancy in sheep. Biol. Reprod. 87, 97.
Maheshwari, A., Fowler, P.A., 2008. Primordial follicular assembly in humans – revisited. Zygote 16, 285–296.
Marques-Pinto, A., Carvalho, D., 2013. Human infertility: are endocrine disruptors to blame? Endocr. Connect. 2, R15–R29.
Matikainen, T., Perez, G.I., Jurisicova, A., Pru, J.K., Schlezinger, J.J., Ryu, H.-Y., Laine, J., Sakai, T., Korsmeyer, S.J., Casper, R.F., Sherr, D.H., Tilly, J.L., 2001. Aromatic hydrocarbon receptor-driven Bax gene expression is required for premature ovarian failure caused by biohazardous environmental chemicals. Nat. Genet. 28, 355–360.
Matsui, Y., Nagano, R., Obinata, M., 2000. Apoptosis of fetal testicular cells is regulated by both p53-dependent and independent mechanisms. Mol. Reprod. Dev. 55, 399–405.
Matzuk, M.M., Dionne, L., Guo, Q., Kumar, T.R., Lebovitz, R.M., 1998. Ovarian function in superoxide dismutase 1 and 2 knockout mice. Endocrinology 139, 4008–4011.
Nagahama, H., Hatakeyama, S., Nakayama, K., Nagata, M., Tomita, K., Nakayama, K., 2001. Spatial and temporal expression patterns of the cyclin-dependent kinase (CDK) inhibitors p27Kip1 and p57Kip2 during mouse development. Anat. Embryol. (Berl.) 203, 77–87.
Pepling, M.E., 2012a. Follicular assembly: mechanisms of action. Reproduction 143, 139–149.
Pepling, M.E., 2012b. Follicular assembly: mechanisms of action. Reproduction 143, 139–149.
Pepling, M.E., Spradling, A.C., 2001a. Mouse ovarian germ cell cysts undergo programmed breakdown to form primordial follicles. Dev. Biol. 234, 339–351.
Pepling, M.E., Spradling, A.C., 2001b. Mouse ovarian germ cell cysts undergo programmed breakdown to form primordial follicles. Dev. Biol. 234, 339–351.
Pepling, M.E., Sundman, E.A., Patterson, N.L., Gephardt, G.W., Medico , L., Wilson, K. I., 2010. Differences in oocyte development and estradiol sensitivity among mouse strains. Reproduction 139, 349–357.
Perez, G.I., Robles, R., Knudson, C.M., Flaws, J.A., Korsmeyer, S.J., Tilly, J.L., 1999a. Prolongation of ovarian lifespan into advanced chronological age by Bax-deficiency. Nat. Genet. 21, 200–203.
Perez, G.I., Robles, R., Knudson, C.M., Flaws, J.A., Korsmeyer, S.J., Tilly, J.L., 1999b. Prolongation of ovarian lifespan into advanced chronological age by Bax-deficiency. Nat. Genet. 21, 200–203.
Phillipps, H.R., Hurst, P.R., 2012. XIAP: a potential determinant of ovarian follicular fate. Reproduction 144, 165–176.
Poljicanin, A., Vukusic Pusic, T., Vukojevic, K., Caric, A., Vilovic, K., Tomic, S., Soljic, V., Saraga-Babic, M., 2013. The expression patterns of pro-apoptotic and anti-apoptotic factors in human fetal and adult ovary. Acta Histochem. 115, 533–540.
Rajareddy, S., Reddy, P., Du, C., Liu, L., Jagarlamudi, K., Tang, W., Shen, Y., Berthet, C., Peng, S.L., Kaldis, P., Liu, K., 2007. p27kip1 (cyclin-dependent kinase inhibitor 1B) controls ovarian development by suppressing follicle endowment and activation and promoting follicle atresia in mice. Mol. Endocrinol. 21, 2189–2202.
Rodrigues, P., Limback, D., McGinnis, L.K., Plancha, C.E., Albertini, D.F., 2008. Oogenesis: prospects and challenges for the future. J. Cell. Physiol. 216, 355–365.
Salnikow, K., Zhitkovich, A., 2008. Genetic and epigenetic mechanisms in metal carcinogenesis and cocarcinogenesis: nickel, arsenic, and chromium. Chem. Res. Toxicol. 21, 28–44.
Shmitova, L.A., 1980. Content of hexavalent chromium in the biological substrates of pregnant women and puerperae engaged in the manufacture of chromium compounds. Gig. Tr. Prof. Zabol., 33–35
Stallock, J., Molyneaux, K., Schaible, K., Knudson, C.M., Wylie, C., 2003. The pro-apoptotic gene Bax is required for the death of ectopic primordial germ cells during their migration in the mouse embryo. Development 130, 6589–6597.
Stanley, J.A., Sivakumar, K.K., Nithy, T.K., Arosh, J.A., Hoyer, P.B., Burghardt, R.C., Banu, S.K., 2013. Postnatal exposure to chromium through mother's milk accelerates follicular atresia in F1 offspring through increased oxidative stress and depletion of antioxidant enzymes. Free Radic. Biol. Med. 61C, 179–196.
Sutton, R., 2010. In: Houlihan, J., Sharp, R., Bruzelius, N. (Eds.), Chromium-6 in U.S. Tap Water. Environmental Working Group, pp. 1–23
Tingen, C., Kim, A., Woodruff, T.K., 2009a. The primordial pool of follicles and nest breakdown in mammalian ovaries. Mol. Hum. Reprod. 15, 795–803.
Tingen, C.M., Bristol-Gould, S.K., Kiesewetter, S.E., Wellington, J.T., Shea, L., Woodruff, T.K., 2009b. Prepubertal primordial follicle loss in mice is not due to classical apoptotic pathways. Biol. Reprod. 81, 16–25.
Wang, Y., Chan, S., Tsang, B.K., 2002. Involvement of inhibitory nuclear factor-κB (NFκB)-independent NFκB activation in the gonadotropic regulation of X-linked inhibitor of apoptosis expression during ovarian follicular development in vitro. Endocrinology 143, 2732–2740.
Wartenberg, H., Ihmer, A., Schwarz, S., Miething, A., Viebahn, C., 2001. Mitotic arrest of female germ cells during prenatal oogenesis. A colcemid-like, non-apoptotic cell death. Anat. Embryol. 204, 421–435.
Xiao, C.W., Ash, K., Tsang, B.K., 2001. Nuclear factor-κB-mediated X-linked inhibitor of apoptosis protein expression prevents rat granulosa cells from tumor necrosis factor α-induced apoptosis. Endocrinology 142, 557–563.
Yamakuchi, M., Lowenstein, C.J., 2009. MiR-34, SIRT1 and p53: the feedback loop. Cell Cycle 8, 712–715.
Zhang, J., Cai, W.W., Lee, D.J., 1992. Occupational hazards and pregnancy outcomes. Am. J. Ind. Med. 21, 397–408.
Zhao, Y., Chaiswing, L., Velez, J.M., Batinic-Haberle, I., Colburn, N.H., Oberley , T.D., Clair, D.K., 2005. p53 translocation to mitochondria precedes its nuclear translocation and targets mitochondrial oxidative defense protein-manganese superoxide dismutase. Cancer Res. 65, 3745–3750.
Ziaee, H., Daniel, J., Datta, A.K., Blunt, S., McMinn, D.J.W., 2007. Transplacental transfer of cobalt and chromium in patients with metal-on-metal hip arthroplasty: a controlled study. J. Bone Joint Surg. 89-B, 301–305.